Fifteenth International Specialty Conference on Cold-Formed Steel Structures
St. Louis, Missouri U.S.A., October 19-20, 2000

15th International Specialty Conference – Cold-Formed Steel Structures 2000

A theoretical and experimental analysis of cold-formed steel shapes subjected to bending – Channel and simple lipped channel

Roberto Martins Gonçalves[1] *Maximiliano Malite*[2] *Carlos Eduardo Javaroni*[3]

EESC – São Carlos School of Engineering, USP – University of São Paulo
Av. Dr. Carlos Botelho, 1465 – CEP 13560-250 – São Carlos, SP, Brazil
Tel. +55.16.273-9455 - Fax. +55.16.273-9482

ABSTRACT

Cold-formed steel shapes have been widely employed in steel construction, where they frequently offer a lower cost solution than do traditional laminated shapes. A classic application of cold-formed steel shapes is purlins in the roof panel of industrial buildings, connected to the roof panel by means of screws. The combined effect of these two elements has been the subject of investigations in some countries. Design criteria were included in the AISI Code in 1991 and 1996.

This paper presents and discusses the results obtained from bending tests carried out on shapes commonly used in Brazil, i.e., the channel and the simple lipped channel. Tests were carried out on double shapes with 4.5 and 6.0 meter spans, which were subjected to concentrated loads and braced against each other on the supports and at intermediary points in three different load situations.

The panel shape was also analyzed experimentally, simulating the action of wind by means of a "vacuum box" designed specifically for this purpose.

The test results were then compared to those obtained through the theoretical analysis, enabling us to extract important information upon which to base proposed design criteria for the new Brazilian code.

[1] Civil Engineer, Doctor's Degree in Structural Engineering, Professor of the Department of Structural Engineering of the EESC-USP. E-mail: goncalve@sc.usp.br
[2] Civil Engineer, Doctor's Degree in Structural Engineering, Professor of the Department of Structural Engineering of the EESC-USP. E-mail: mamalite@sc.usp.br
[3] Civil Engineer, Doctor's Degree in Structural Engineering, Professor of the Civil Engineering Department of UNESP, Bauru campus. E-mail: javaroni@bauru.unesp.br

INTRODUCTION

Cold-formed steel shapes are widely employed as structural elements in the most varied types of steel construction in Brazil. Some examples of their use as framing members are warehousess for a wide variety of uses, residential, commercial or industrial coverings, and low-rise residential buildings. Some examples of isolated structural elements are purlins, longitudinal beams and diagonal bracing elements.

As for the materials used in Brazil, it can be observed that many structures are produced using steel shapes with non-structural quality, the steels having SAE (Society of Automotive Engineers) classification. Although of common quality and easily available in the market, with structural performance proven through experience, these steels carry no guarantee in terms of their physical and mechanical characteristics.

As for the regulating aspects, the Brazilian code on dimensioning of cold-formed shapes, "Calculation of Steel Structures Constituted of Light Shapes", NB143, ABNT (1967) published in 1967, is outdated and in disuse. Along the last thirty years and with the growing use of cold-formed shapes for structural purposes, designers have found it necessary to resort to foreign codes, principally those of the American Iron and Steel Institute, AISI.

Research work in the area of steel structures in Brazil has expanded in recent years, contributing significantly to the growing use of steel in Brazilian civil construction and toward the educational improvement and qualification of the professionals whose activities focus on the design and building of these structures.

To achieve these improvements, the activities in the area of metal structures of the Department of Structural Engineering, São Carlos School of Engineering have, in the past few years, focused on incrementing research in steel structures. As a result of this research work, the area of metal structures has been engaged in coordinating the revision and updating of the NB 143, ABNT (1967) code, which should culminate in a new edition of the Brazilian code for the design of cold-formed structural steel structural elements.

This work, which is part of a series of research projects on the use and application of steel in Brazilian metal construction, presents the findings of tests carried out on cold-formed steel shapes with cross sections of the channel and simple lipped channel types, as well as the results of the tests of these steel shapes in roof panel systems tested in a "vacuum box" to simulate the effect of wind suction on roof panels. These tests were developed at the Structural Lab of the Structural Engineering Department, São Carlos School of Engineering.

MATERIAL

The 2.25mm and 3.00mm-thick steel sheets used in this research work, commercially known as USI-SAC 41, were supplied by USIMINAS S.A., a Brazilian metallurgic company.

To determine the characteristics of steel strength, tests were performed on 12 (twelve) specimens prepared according to the ASTM A370 specification, determining the tensile yield point (F_y) and the tensile strength (F_u), for which three specimens each were taken from four different steel sheets.

Table 1 presents the results obtained from these tests. Elongation was measured on the measurement basis of 50mm. All the specimens presented a defined yield level and the value of the modulus of elasticity (E) was 205,000 MPa, a normative value for steel.

TABLE 1 – Mechanical characteristics of the steel used.

Test	A (mm^2)	Elongation (mm)	Ny (kN)	Nu (kN)	Elongation (%)	F_y (Mpa)	F_u (Mpa)
1A	38.130	68.42	13.40	17.45	36.84	351.43	457.64
1B	37.324	67.15	13.00	17.00	34.30	348.30	455.47
1C	38.440	66.75	13.10	17.30	33.50	340.79	450.05
2A	28.125	66.56	9.80	13.35	33.12	348.44	474.67
2B	27.630	64.95	9.85	13.00	29.90	356.50	470.50
2C	27.540	64.45	9.85	13.10	28.90	357.66	475.67
3A	28.409	66.85	9.45	13.10	33.70	332.64	461.12
3B	27.725	65.96	9.30	12.85	31.92	335.44	463.48
3C	28.181	65.91	9.55	13.10	31.82	338.88	464.86
4A	39.122	68.43	13.40	17.80	36.86	342.52	454.99
4B	38.626	66.08	42.70	17.40	32.16	328.79	450.47
4C	38.440	65.12	13.00	17.60	30.24	338.19	457.86
Mean value					32.77	343.30	461.40
Standard deviation					2.50	9.23	8.69

NORMATIVE ASPECTS

In its most recent versions, the American Iron and Steel Institute (AISI), a specific code on the design of cold-formed steel structural members, still determines the strength of cold-formed steel beams according to the results of the work of Winter (1943, 1944 and 1959).

The theoretical solution of Timoshenko, Gere (1961) for a simply supported "I" beam under equal moment, equation (1), has been employed as a reference.

$$M_{cr} = \frac{\pi}{L}\sqrt{EI_y GI_t\left(1+\frac{\pi^2 EC_\omega}{GI_t L^2}\right)} \qquad (1)$$

The effects of the moment gradient and the several support conditions, on the other hand, are adjusted by means of an empirical modification factor applied to the results obtained by Timoshenko, Gere (1961). This approximation has been used for over 50 years.

Approximate formulas for the moment modification factor, (C_b), have been presented by several researchers.

Salvadori (1955, 1956) solved the problem of an "I" type beam under equal moment using the Raleigh-Ritz method, considering several terms in the development in series of the expressions of lateral displacement and rotation. Later, the SSRC (Structural Stability Research Council) approximated those results using the following expression:

$$C_b = 1.75 + 1.05r + 0.3r^2 \leq 2.3 \tag{2}$$

Throughout the past years, several formulations assuming different hypotheses and support conditions have been published and discussed.

According to Pandey, Sherbourne (1989) and Sherbourne, Pandey (1989), the results of these studies have been similar inasmuch as they either failed to include or simply approximated the torsional warping constant for the sake of analytical simplicity. From this standpoint, the work presents a theoretical solution for lateral torsional buckling of "I" beams in the elastic regime, considering the problem as a superimposition of two hypothetical cases, one corresponding to warping equal to zero and the other having torsional stiffness equal to zero.

Salvadori's expression was used by the AISI up to its 1991 edition, after which its 1996 edition suggests the use of a new expression for C_b, based on the studies of Kirby and Nethercot:

$$C_b = \frac{12.5M_{max}}{2.5M_{max} + 3M_A + 4M_B + 3M_c} \tag{3}$$

where:

M_{max} = absolute value of maximum moment in the unbraced segment.

M_A = absolute value of moment at quarter point of unbraced segment.

M_B = absolute value of moment at centerline of unbraced segment.

M_C = absolute value of moment at three-quarter point of unbraced segment.

When cross loads are applied excentrically in relation to the shear center, the equations M_{cr} and C_b differ from those mentioned earlier.

The influence of contour and load conditions on the instability of single symmetric sections is, on the other hand, less known than the influence of these conditions on double symmetric sections.

Kavanagh and Ellifritt (1994), based on their results of tests on simple lipped channel shapes, concluded that the AISI equations may overestimate the lateral buckling strength, particularly in cases where there are two or more intermediary lateral braces. According to these authors, the tests demonstrated the occurrence of failure by distortion at the intersection of the flange and the stiffener at the locked points.

For isolated shapes, which are subject to lateral buckling with torsion, the flexural strength, according to the AISI (1996), is obtained by means of the following expression:

$$M_n = S_c \frac{M_c}{S_f} \tag{4}$$

where:

S_f = Elastic section modulus of the unreduced section for the extreme compressive fiber.

S_c = Elastic section modulus of the effective section calculated at a stress M_c/S_f in the extreme compression fiber.

M_c = Critical moment calculated according to Equation (5), Equation (6) or Equation (7).

For $M_e \geq 2.78M_e$

$$M_c = M_y \tag{5}$$

For $2.78M_y > M_e > 0.56M_y$

$$M_c = \frac{10}{9} M_y \left(1 - \frac{10M_y}{36M_e}\right) \tag{6}$$

For $M_e \leq 0.56M_y$

$$M_c = M_e \tag{7}$$

M_y is the moment causing initial yield at the extreme compression fiber of the full section and M_e is the elastic critical moment computed by Equation (8) for bending about the symmetry axis (x-axis is the axis of symmetry):

$$M_e = C_b r_0 A \sqrt{\sigma_{ey} \sigma_t} \tag{8}$$

where:

C_b = Bending coefficient.

r_0 = Polar radius of gyration of the cross section about the shear center.

A = Full cross-sectional area.

L_y, L_t = Unbraced length of compression member for bending about the y-axis and for twisting.
K_y, K_t = Effective length factors for bending about the y-axis and for twisting.

For flexural members with a flange connected to a panel, lateral buckling no longer occurs in the transversal section as a whole. Flexural strength is less than that of a laterally braced member, although it is higher than that of a laterally unbraced member. In this case, the partial restriction caused by the panel can be represented by a reduction factor obtained by the ratio between the moment that causes the initiation of yield of the extreme compression fiber (M_y) and the ultimate moment (M_u) observed in the tests, equation (5), Johnston, Hancock (1994); LaBoube (1992); LaBoube (1992); Murray, Elhouar (1994).

$$R = \frac{M_u}{M_y} \tag{9}$$

The values of R, according to the AISI (1996, 1991), are:

R=0.40 for simple span C sections;
R=0.50 for simple span Z sections;
R=0.60 for continuous span C sections;
R=0.70 for continuous span Z sections.

TESTS ON FLEXURE MEMBERS

The flexure tests were carried out on channel and simple lipped channel type shapes with spans, loads and lateral bracing chosen so as to initiate the occurrence of the local buckling and global buckling failure modes in the tested shapes.

The cross sections and their nominal dimensions are shown in Figure 1. The sheet thicknesses used were 2.25 mm and 3.0 mm.

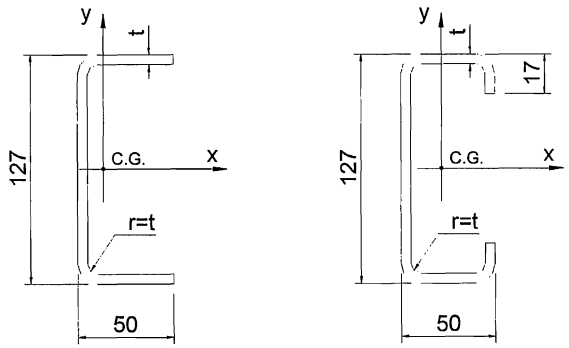

Figure 1: Cross-Section Dimensions.

The shapes were subjected to two different spans under three different load situations, as illustrated in Figure 2. The intermediary lateral bracing is indicated in this figure by an x, and this bracing was done between two shapes , which were tested in pairs.

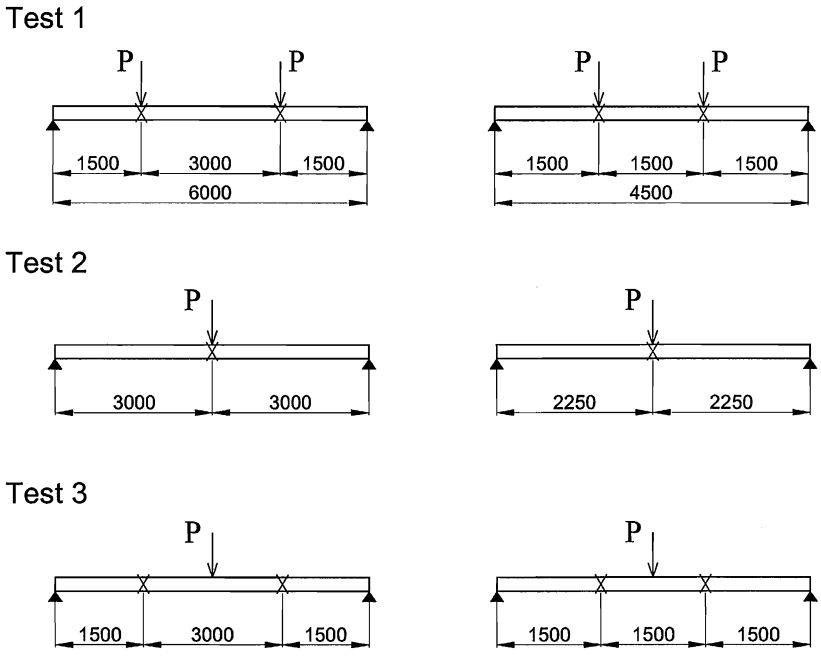

Figure 2: Test Geometry.

Figure 3 shows the application of loads, the load cell, the hydraulic jack and the displacement transducers positioned for testing.

Figure 4 shows the arrangement used for the supports and the lateral bracing of the shapes. Details of that are given in Javaroni(1999).

The strains that occurred were measured at the cross section in mid-span, as illustrated in Figure 5.

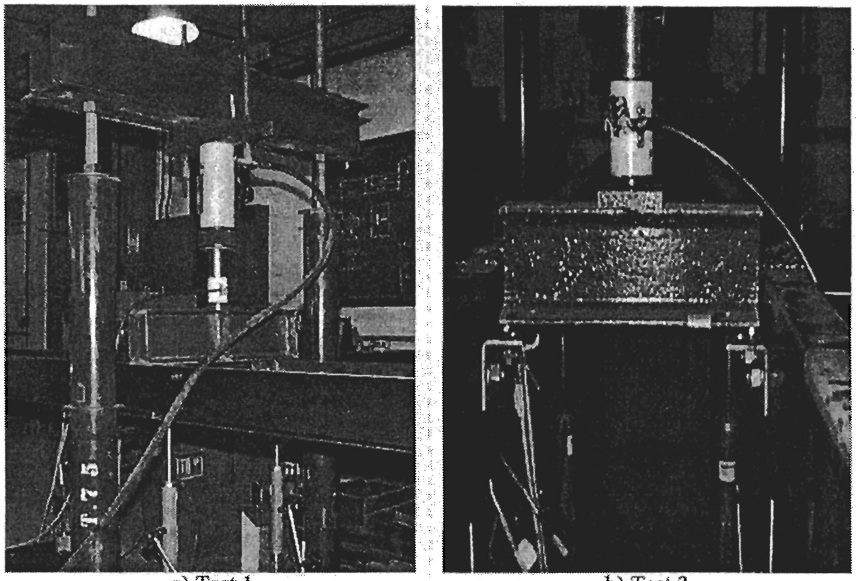

a) Test 1 b) Test 3

Figure 3: Examples of load applied.

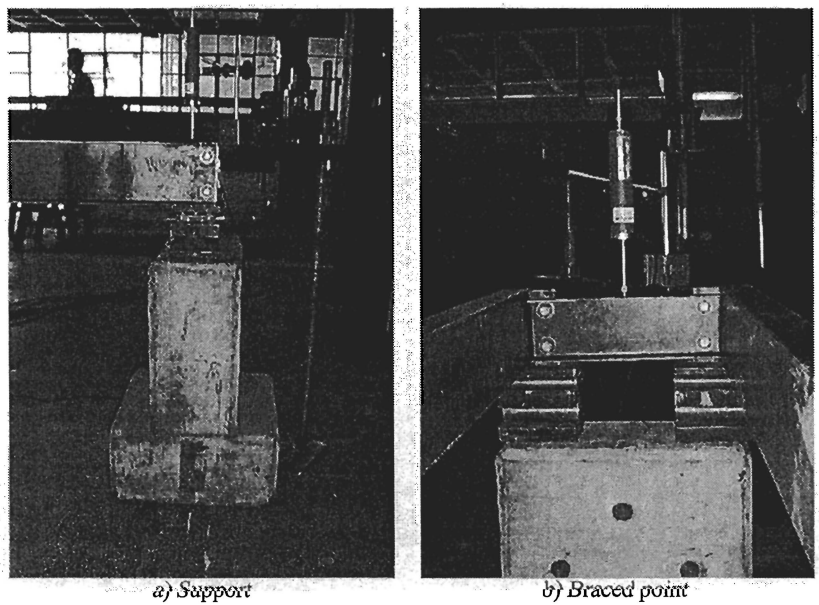

a) Support b) Braced point

Figure 4: Arrangements for tests.

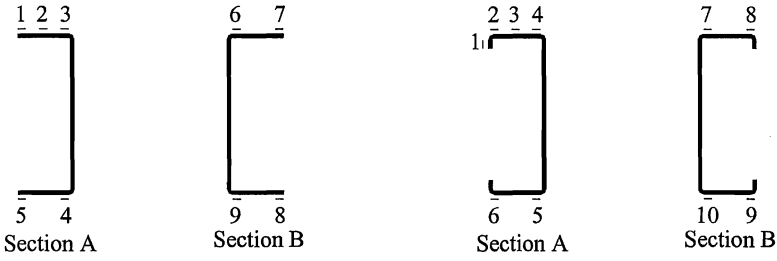

Figure 5: Position of the strain gages at the cross sections.

Table 2 shows the results of ultimate load obtained from the tests, the observed failure mode and the failure mode foreseen according to the AISI prescriptions.

It can be observed from this table that the foreseen and actual failure modes differ for some of the sets tested.

The rotation in the cross section and the horizontal displacements modify the distributions of stresses in the flange, preventing a uniform distribution, as can be observed in the graph of figure 6, which corresponds to the U2 set.

In this test (U2), local buckling occurred in the region approximately 0.5 meter away from the braced point, leading to an effective torsional buckling length of 1 meter, which resulted in $K_t \cong 0.5$.

In the same way that the rotation altered the distribution of stresses along the flange in the cross section at mid-span, the rotation at the extremities occurred in the opposite direction, in this case increasing the compressive stress on the free edge and justifying the occurrence of local bending of this part where the moment and, consequently, the normal corresponding stresses, are lesser.

Table 3 gives the mean values obtained from the tests and those obtained from the AISI/96 prescriptions, using the values $K_t=0.5$ and $K_y \cong 1.0$.

Table 1: Results obtained in the flexure tests.

	Test	Shape	Situation	Span (m)	P_{ult} (kN)	M_{ult} (kN.m)	Observed Failure (Foreseen Failure)
	U1	U127x50x2.25	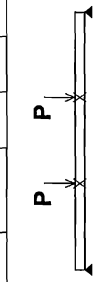	6	3.77	3.77	LB (LB)
	U2				4.18	4.18	LTB (LB)
	U3	U127x50x3.0		6	6.53	6.53	LTB (LB)
	U4				6.04	6.04	LTB (LB)
T	U5	U127x50x17x2.25		6	6.59	4.94	LB (LTB)
E	U6				6.96	5.22	LB (LTB)
S	U7	U127x50x3.0		6	6.16	4.62	LTB (LTB)
T	U8				6.80	5.10	LTB (LTB)
	U9				6.03	4.52	LB (LTB)
1	U10	U127x50x2.25		6	4.52	3.39	LB (LB)
	U11				4.31	3.23	LB (LB)
	U19	U127x50x3.0		4.5	9.95	7.46	LB (LB)
	U20				10.89	8.17	LB (LB)
	U21				10.88	8.16	LB (LB)
	U12	U127x50x3.0	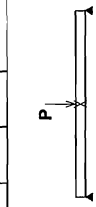	6	7.91	5.93	LTB (LTB)
	U13				7.81	5.86	LTB (LTB)
T	U14				7.86	5.90	LTB (LTB)
E	U15	U127x50x2.25		6	5.23	3.92	LTB (LTB)
S	U16				5.18	3.88	LTB (LTB)
T	U17	U127x50x17x3.0		6	10.81	8.11	LTB (LTB)
	U18				10.94	8.20	LTB (LTB)
2	U22	U127x50x3.0		4.5	13.51	7.60	LTB/LB (LTB)
	U23				13.33	7.50	LTB (LTB)
	U24				13.51	7.60	LTB/LB (LTB)
T	U25	U127x50x3.0	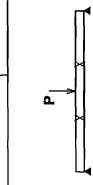	4.5	13.90	7.82	Equipament failure
E	U26				15.55	8.75	LB (LB)
S	U27				15.50	8.72	LB (LB)
T	U28	U127x50x3.0		6	8.58	6.44	LTB (LTB)
	U29				8.53	6.40	LTB (LTB)
3	U30				9.04	6.78	LTB (LTB)

Notes: a) The values of $P_{ultimate}$ refer to the tested set. Hence, for the individually tested shape, the value to be considered should be one half. b) $M_{ultimate}$ corresponds to the individual shape. c) LB: Local Buckling. d) LTB: Lateral-Torsional Buckling. e) The U1 and U2 sets were tested with loads at every 1/3 of the span. f) 1 in = 25.4 mm and 1 ksi = 6.895 MPa.

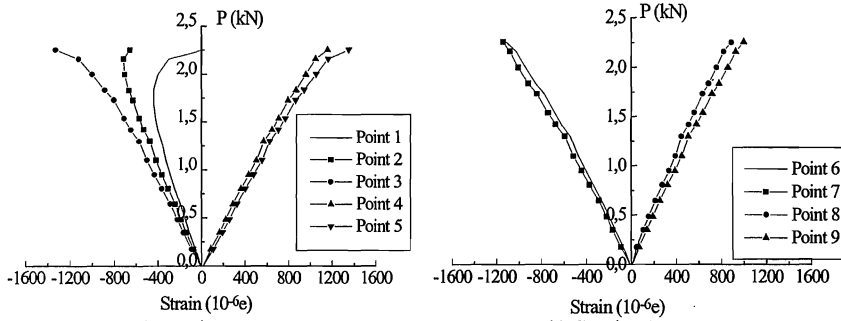

Figure 6: Applied load vs. strain – Set U2.

Table 3: Comparison of the results obtained (K_t=0.5 ; K_y=1.0).

Section	Span (m)	Test (number)	P_{ult} (kN)	P_{AISI} (kN)	P_{ult}/P_{AISI} (kN)
U127x50x3.00	6.0	1	6.32	5.73	1.103
		2	7.86	7.84	1.003
		3	7.99	6.05	1.321
U127x50x3.00	4.5	1	10.57	9.44	1.120
		2	13.45	11.11	1.211
		3	15.17	12.83	1.182
U127x50x2.25	6.0	1	4.39	3.60	1.219
		2	5.20	5.37	0.968
U127x50x17x2.25	6.0	1	6.78	7.18	0.944
U127x50x17x3.00	6.0	2	10.87	10.28	1.057
U127x50x3.00	6.0	1**	6.28	5.85	1.073
U127x50x2.25	6.0	1**	4.12	3.84	1.073
Z127x50x17x2.25	6.0	1**	5.86	5.30	1.106

*Mean values obtained for the tested sets.
**Loads applied at every 1/3 of the span.

TESTS ON BEAMS HAVING ONE FLANGE CONNECTED TO SHEATING

Figure 7 shows the cross sections of the analyzed shapes.

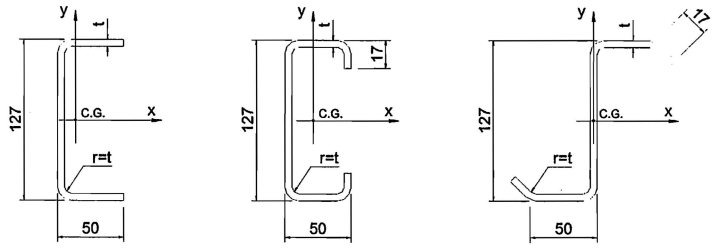

Figure 7: Cross sections for the purlins.

Testing was carried out in a device called a "vacuum box", which consists of a box whose design dimensions may vary from 3m x 6m up to 12m x 6m, in 1m x 6m modules. Its lateral faces and bottom are made of 21mm-thick plywood. The frame is made of cold-formed steel shapes, as illustrated in figure 8.

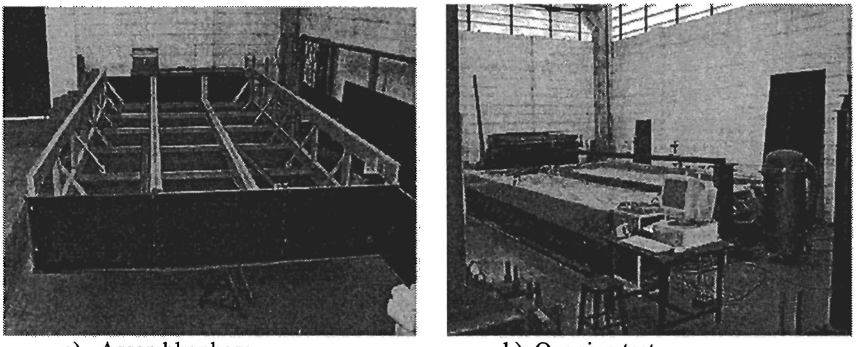

a) Assembly phase. b) Ongoing test.

Figure 8: Vaccum box.

The upper part of the box consists of the roof tile-purlin set one wishes to test, placed in an inverted position from that of conventional roof so that, as the air inside the box is removed, the difference between the internal and external pressures exert an overpressure on the set, simulating the suction effect of wind. This difference between pressures is distributed uniformly on the entire surface of the panel formed by the roof tiles. Assembling the set in the inverted position allows for a visual verification of the behavior of the shape and facilitates instrument placement and data collection.

The steel tiles employed had a 4,010 mm-long trapezoidal cross section whose characteristic dimensions are indicated in figure 9.

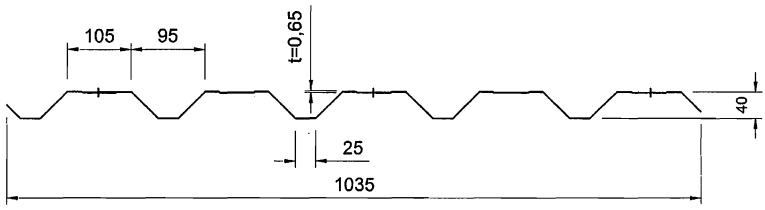

Figure 9: Cross section of the steel roof tile in the assembly position.

A total of 15 tests were carried out with three different types of cross sections for the shapes. Seven of these tests were carried out without sag rods and 8 with two sag rods, one at every 1/3 of the span, as indicated in table 4.

Table 4: Tested shapes.

Test	Shape	Sag rods
1	U127x50x3.00	No
2	U127x50x17x3.00	No
3	Z127x50x17x3.00	No
4	U127x50x3.00	No
5	U127x50x3.00	No
6	U127x50x17x3.00	No
7	U127x50x17x3.00	No
8	U127x50x2.25	1/3 of the span
9	U127x50x2.25	1/3 of the span
10	U127x50x2.25	1/3 of the span
11	U127x50x3.00	1/3 of the span
12	Z127x50x17x2.25	1/3 of the span
13	Z127x50x17x2.25	1/3 of the span
14	Z127x50x3.00	1/3 of the span
15	Z127x50x3.00	1/3 of the span

Figure 10 illustrates the placement of the sag rods at the purlins and fixing of the roof tiles to the shapes, using self-threading screws.

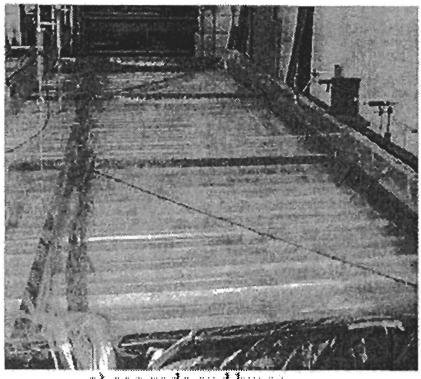

a) sag rods and brace

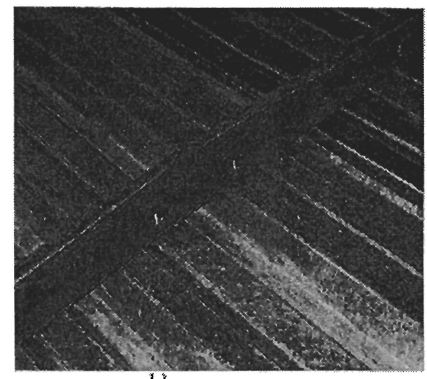

b) screws

Figure 10: Sag rods for the purlins.

Table 5 gives the results of the pressure applied in the tests. This pressure refers to the relative value of displacement in the mid-span equal to 1/100 of the span (56.2 mm). The use of this value is justified as being that for which the damage of the structure is had, hence characterizing its failure. The value of the moment in the mid-span section, M_{ref}, corresponds to the value of the pressure for 1/100 of the span. This moment is one of uniformly distributed load along the length of the shape, whose value is obtained by the product between the value of the reference pressure and the influence width for the shape. This influence width was determined based on the vertical displacements measured at half span for the lateral shapes and for the instrumented shape.

Table 5: Reference pressure for the purlins.

Test	Shape	Sag rods	p (kN/m^2)	M_{ref} (kN.m)
1	U127x50x3.00	No	0.85	4.30
2	U127x50x17x3.00	No	0.93	5.65
3	Z127x50x17x3.00	No	0.80	3.60
4	U127x50x3.00	No	0.61	3.09
5	U127x50x3.00	No	0.50	2.53
6	U127x50x17x3.00	No	0.55	2.78
7	U127x50x17x3.00	No	0.52	2.15
8	U127x50x2.25	1/3 of the span	0.75	4.74
9	U127x50x2.25	1/3 of the span	0.65	4.41
10	U127x50x2.25	1/3 of the span	0.75	4.62
11	U127x50x3.00	1/3 of the span	1.00	6.87
12	Z127x50x17x2.25	1/3 of the span	0.80	5.81
13	Z127x50x17x2.25	1/3 of the span	0.80	5.81
14	Z127x50x17x3.00	1/3 of the span	0.96	8.03
15	Z127x50x17x3.00	1/3 of the span	0.98	8.20

The types of failure that occurred for the shapes connected to the roof tiles were excessive displacement and local buckling of the flange, possibly associated to distortion. In the case of the shapes without sag rods, already evident for the low pressure values, induced early failures in the element. This is important and should be analyzed as a possible failure mode for the purlins for which sag rods are not used. Figure 11 illustrates this phenomenon.

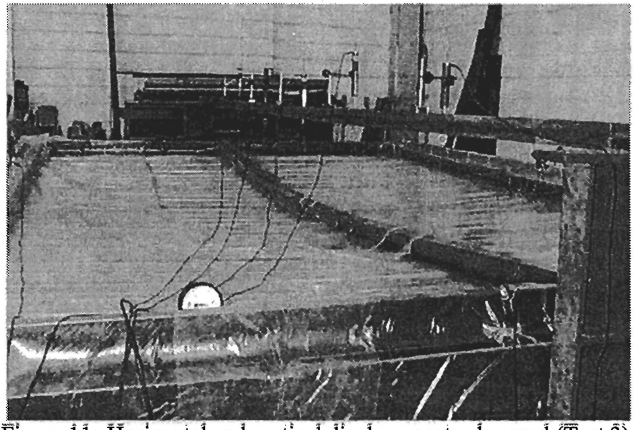

Figure 11: Horizontal and vertical displacements observed (Test 3).

Figure 12 presents the strains corresponding to the U127x50x17x3.0 type shape, test 7, measured at the cross section in mid-span. In this test, in addition to the strains in the flanges, figure 12a, measurements were also taken along the web of the shape, the results of which are given in figure 12b.

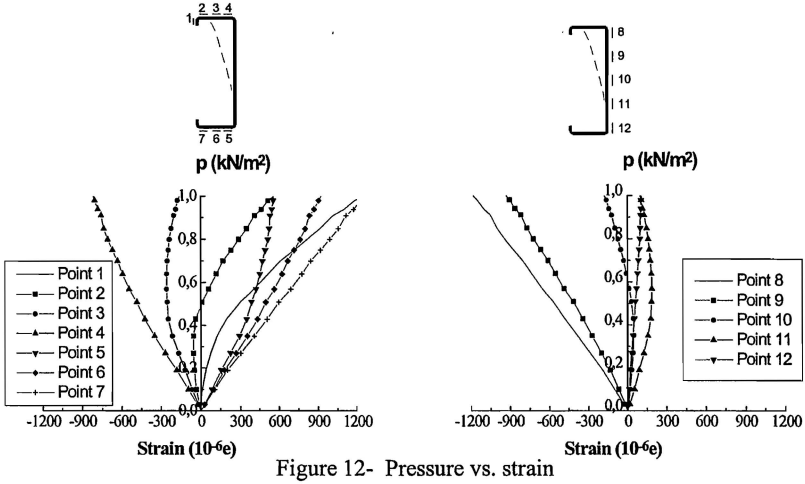

Figure 12- Pressure vs. strain

An observation of the strains that occurred in the cross section at mid-span lead to some important considerations. This graph shows the decrease in strains, in absolute values, for points 2, 3 and, less pronouncedly, for point 5.

This decrease is due to the high rotation of the cross section close to the joint of the web with the tractioned flange, leading to the appearance of tension near the stiffeners and compressive stresses in the region of the web and causing the variation in the distribution of stresses in the cross section of the shape. This finding is in agreement with the hypotheses adopted by the Peköz, Soroushian (1982) model, in which the stresses in the cross section are computed assuming the superimposition of two different stages: the first due to vertical displacement and the second one due to horizontal displacement and cross sectional rotation.

This evidence was found for all the shapes without sag rods, although it was more strongly marked for the channel type shapes.

The behavior of the shapes braced by sag rods is quite different from that in which these elements are not used. As observed earlier, for the shapes without sag rods, the horizontal displacements begin concomitantly to loading while, in the presence of sag rods, these displacements remain practically absent nearly up to the ultimate load.

Figure 13 shows the behavior of pressure versus strain for a U127x50x3.0 type shape, which corresponds to test 11, and is representative of the behavior of the shapes tested with sag rods.

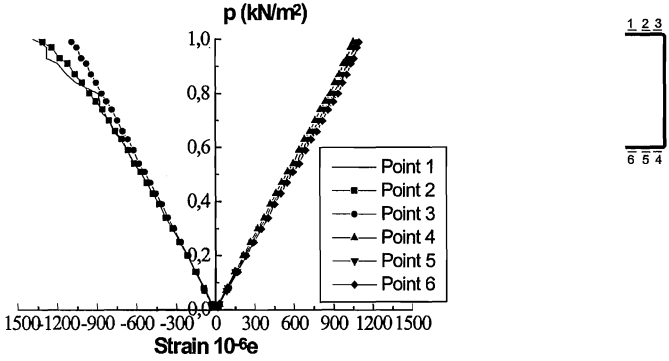

Figure 13 - Pressure vs. strain – Test 11, with sag rods.

Figure 14 presents illutrative photographs of the rupture that occurred in the system in two different situations. The first photograph, figure 14a, shows the failure for a pilot test while figure 14b illustrates the failure that occurred in test 11.
The presence of sag rods almost entirely prevents horizontal displacement of the compressed flange. Therefore, these purlins can be analyzed considering only the effects of simple flexure.

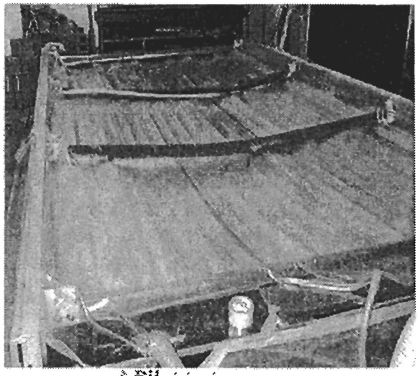

a) Pilot test

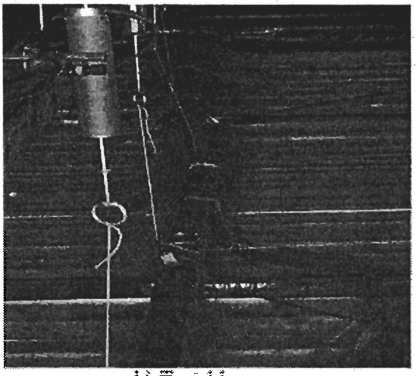

b) Test 11

Figure 12: Examples of failures observed for the purlins.

The F_R value, Table 6, expresses the ratio between the flexural strength in test and the moment of initial yielding based on the elastic section modulus of the effective section.

Table 6 – Ultimate and yield moments.

Test	Shape	p (kN/m²)	M_{ref} (kN.m)	M_y (kN.m)	$F_R=M_u/M_y$
Without sag rods					
1	U127x50x3.00	0.85	4.30	7.52	0.57
2	U127x50x17x3.00	0.93	6.54	9.28	0.70
3	Z127x50x17x3.00	0.80	3.60	10.16	0.35
4	U127x50x3.00	0.61	3.09	7.42	0.42
5	U127x50x3.00	0.50	2.53	7.42	0.34
6	U127x50x17x3.00	0.55	3.86	9.28	0.42
7	U127x50x17x3.00	0.52	3.65	9.28	0.39
With sag rods					
8	U127x50x2.25	0.75	4.74	5.21	0.91
9	U127x50x2.25	0.65	4.41	5.21	0.85
10	U127x50x2.25	0.75	4.62	5.21	0.89
11	U127x50x3.00	1.00	6.87	7.42	0.92
12	Z127x50x17x2.25	0.80	5.81	7.46	0.78
13	Z127x50x17x2.25	0.80	5.81	7.46	0.78
14	Z127x50x17x3.00	0.96	8.03	9.77	0.82
15	Z127x50x17x3.00	0.98	8.20	9.77	0.84

Note: p(kN/cm²) indicates the value of the applied pressure corresponding to the displacement equal to 1/100 of the span (56.2 mm). For this pressure value, the value of the M_{ref} moment was determined.

The average values of the results obtained were:

Channel type without sag rods: $F_R = 0.50$
Simple lipped channel type without sag rods: $F_R = 0.50$
Channel type with 2 sag rods: $F_R = 0.89$
Z section with 2 sag rods: $F_R = 0.80$

It should be pointed out that these values should be restricted to the conditions used in the tests described herein and that their extrapolation to other situations is subject to possible errors in assessment of the flexural strength.

Only one test was carried out for the Z section without sag rods; therefore, the value obtained (F_R=*0.35*) cannot be considered representative of this tipe of shape. These values were compared to the results of 25 other tests performed by LaBoube (1992, 1991) and Peköz, Soroushian (1982) together with those developed by Javaroni (1999). One can conclude, therefore, that the values presented herein practically reproduce the mean values and standard deviations obtained by LaBoube.

In addition, the value of F_R=*0.40* for channel type shapes proved to be appropriate for shapes both with stiffened and with unstiffened flanges.
In an earlier evaluation (Javaroni, 1999), the Peköz, Soroushian (1982) method presented results of normal stresses that were coherent with the strains measured in the cross sections of the tested shapes. However, the values of the spring stiffness coefficient (K) varied considerably and the determination of a theoretical value for design purposes requires a deeper study owing to the various parameters involved. It should also be pointed out that specific testing procedures exist to determine this coefficient. An advantage of the Eurocode (1993) procedure is that it provides an analytical expression to determine the spring stiffness coefficient.

CONCLUSIONS

This study analyzed cold-formed steel shapes whose cross sections, specifically the channel type, are widely employed in steel construction in Brazil.

For the isolated shapes, the results calculated by means of the AISI (1996) procedure proved satisfactory, provided buckling coefficient values are used that are appropriate for the details of the lateral bracing employed.

It was observed that unforeseen limit states occurred in some of the tests, which may be associated to the closer proximity of the laterally braced points, where the stress gradient in the compressed flange resulting from the rotation of the cross section may inhibit local buckling of the flange. On the other hand, this same gradient may superimpose the compressive stresses, leading to possibly unforeseen local buckling of the flange.

The experimental analysis of the shapes connected to the steel roof tiles was carried out in two stages: purlins without sag rods and purlins 2 two sag rods.

Tests carried out on the purlins showed differing behaviors for the shapes with and without the use of sag rods.

In the absence of sag rods, the purlins presented a failure mode resulting from excessive horizontal displacement of the compressed flange, which was found to occur in all the

tested cross sections. This fact, characterizing the ultimate limit state of purlins without sag rods, is considered of crucial importance and should be seen as a failure mode for future study, for which a mathematical model suitable to the behavior of the shape must be found.

The use of the reduction factor proved to be a fairly simple procedure for use in routine design, however, it is subject to the conditions used in tests and its extrapolation may lead to gross errors.

When sag rods are used, the shapes present practically no horizontal displacement of the compressed flange, showing only vertical displacements. This finding suggests that purlins should be analyzed as bars subject to simple flexure. The sag rods also allowed for a gain in purlin strength, which was represented by the increased ultimate pressure in the "vaccum box".

ACKNOWLEDGMENTS

The authors gratefully acknowledge the Brazilian research funding institution FAPESP for its financial support of this research project, and USIMINAS S.A. for the donation of the steel used to conform the shapes for testing.

REFERENCES

AMERICAN IRON AND STEEL INSTITUTE (1996) **Cold formed steel design manual.** AISI, Washington.

AMERICAN IRON AND STEEL INSTITUTE (1991) **LRFD Cold formed steel design manual.** AISI, Washington.

ASSOCIAÇÃO BRASILEIRA DE NORMAS TÉCNICAS. (1967) **Calculation of Steel Structures Constituted of Light Shapes; NB-143.** ABNT, Rio de Janeiro. 31p.

JAVARONI, C. E. (1999) **Cold-formed steel members in flexure: theoretical-experimental analyses.** São Carlos, 1999. 255p. Thesis. São Carlos School of Engineering, University of São Paulo.

JONHSTON, N.; HANCOCK, G. (1994) **Calibration of the AISI R-factor design approach for purlins using Australian test data.** Engineering Structures, v.16, n.5, p.342-347.

KAVANAGH, K. T.; ELLIFRITT, D. S. (1994) **Design strengths of cold-formed channels in bending and torsion.** Journal of Structural Engineering, ASCE, v.120, n.5, p.1599-1607, May.

LaBOUBE, R. A. (1992) **Estimating uplift capacity of light steel roof system.** Journal of Structural Engineering, ASCE, v.118, n.3, p.848-852, Mar.

LaBOUBE, R. A. (1991) **Uplift capacity of Z-purlins.** Journal of Structural Engineering, ASCE, v.117, n.4, p.1159-1166, April.

PANDEY, M. D. SHERBOUNE, A. N.; (1989) **Unified v. integrated approaches in lateral-torsional buckling of beams.** The Structural Engineer, v.67, p.245-249, July.

PEKÖZ, T.; SOROUSHIAN, D. (1982) **Behavior of C and Z purlins under uplift.** Sixth International Specialty Conference on Cold-Formed Steel Structures, p.409-429, St. Louis, Missouri, USA. *Proceedings*.

SALVADORI, M. G. (1955) **Lateral buckling of I beams.** Transactions, ASCE, v.120, p.1165-1177.

SALVADORI, M. G. (1956) **Lateral buckling of eccentrically loaded I columns.** Transactions, ASCE, v.121, p.1163-1178.

SHERBOUNE, A. N.; PANDEY, M. D. (1989) **Elastic, lateral-torsional stability of beams: moment modification factor.** Journal of Constructional Steel Research, v.13, p.337-356.

TIMOSHENKO, S. P.; GERE, J. M. (1961) **Theory of elastic stability.** 2.ed. New York: McGraw-Hill. 541p.

WINTER, G. (1959) **Cold-formed, light-gage steel construction.** Journal of the Structural Engineering, ASCE, v.85, n.ST9, p.151-173, Nov.

WINTER, G. (1944) **Strength of slender beams.** Transactions, ASCE, v.109, p.1321-1349.

WINTER, G. (1943) **Lateral stability of unsymmetrical I-beams and trusses in bending.** Transactions, ASCE, v.108, p.247-260.

APPENDIX - NOTATION

A = Full unreduced cross-sectional area of the member
C_b = Bending coefficient dependent on moment gradient
C_w = Torsional warping constant of the cross-section
E = Modulus of elasticity of steel, 205 000 Mpa
F_y = Tensile yield point
F_u = Tensile strength
G = Shear modulus of steel
I_x, I_y = Moment of inertia of full section about principal axis
I_t = St. Venant torsion constant
K_t = Effective length factor for torsion
K_y = Effective length factor for buckling about y-axis
L = Full span for simple beams
L_t = Unbraced length of compression member for torsion
L_y = Unbraced length of compression member for bending about y-axis
M_{max}, M_A, M_B, M_C = Absolute value of moments in an unbraced segment, used for determining C_b
M_c = Critical moment
M_e = Elastic critical moment
M_y = Moment causing a yield strain
P_{ult} = Load test
p = Pressure in "vacuum box"
R = Reduction factor
r_0 = Polar radius of gyration of the full cross-section about the shear center
t = Thickness of section